Pergamon

PII: S0191-8141(96)00107-1

Journal of Structural Geology, Vol. 19, Nos 3–4, pp. 321 to 335, 1997

0191-8141/97 $17.00 + 0.00

Multiple geometries and modes of fault-propagation folding in the Canadian thrust belt

ERIC A. ERSLEV and KYLE R. MAYBORN*

Department of Earth Resources, Colorado State University, Fort Collins, CO 80523, U.S.A.

(*Received* 27 *February* 1996; *accepted in revised form* 11 *November* 1996)

Abstract—A multitude of fold models have been proposed to explain the variety of fold geometries which develop in front of thrust faults. Detailed field, fabric, and photogrammetric studies of 4 fault-cored asymmetrical folds in the thin-skinned Canadian thrust belt were used to test models of fault-propagation folding. Fold geometries include combinations of angular and rounded fold surfaces, highly contorted anticlinal hinge areas, and minimal penetrative deformation or changes in bedding thickness. Interlimb angles generally decrease with increasing shortening, indicating progressive fold tightening about fixed anticlinal hinges. Extensive flexural slip thrusting toward the anticlinal axes of angular folds suggests that kink folding in thin-skinned thrust belts is aided by material transfer from both fold limbs into hinge areas. Fold geometries change dramatically along the strike of individual structures, demonstrating the non-uniqueness of fault-propagation fold geometries.

No single mode of fault-propagation folding can explain the diverse fold geometries seen in the Canadian thrust belt. This geometric variability can be ascribed to the complex interplay of multiple modes of folding. In strata near the causal thrusts, oblique shear and flexural slip in triangular shear zones distribute thrust displacements into both rounded and angular folds. Simultaneous angular folding of overlying strata commonly occurs by progressive kink folding where folds tighten by flexural slip on all fold limbs until the thrust breaks through the fold. Regional and local differences in the amount of pervasive, top-to-the-craton shear needed for progressive kink folding may be partially responsible for the variability of fault-propagation fold geometries in thin- and thick-skinned orogens world-wide.

INTRODUCTION

Both thin- and thick-skinned thrust belts show the intimate relationship between folding and faulting where the steep forelimbs of asymmetrical folds are cut by thrust faults. Many of these structures have been called fault-propagation folds, which were defined by Suppe (1985) as folds that "represent deformation that takes place just in front of the propagating fault surface". A multiplicity of conceptual and quantitative models for fault-propagation folding have been proposed to explain the corresponding diversity of structural geometries. These models have important implications to our knowledge of the geometry and internal structure of petroleum reservoirs as well as the seismic hazard of areas (e.g. Northridge, California) underlain by active fault-related fold structures.

We recognize that the term 'fault-propagation folding' was initially coined to describe structures in thin-skinned thrust belts and that some authors further restrict the term to "a geometric, kinematic model that explicitly describes the evolution of a tip-line fold using equations relating fold geometry to fault shape and displacement" (Fischer *et al.*, 1992). But we choose to view the term as a kinematic concept describing the wave of deformation preceding a propagating fault (J. Suppe, personal communication, 1995), not a rigidly-defined kinematic framework. The similarity of the fault-propagation fold definition from thin-skinned orogens and the 'thrust-fold' definition (Stone, 1984) from thick-skinned orogens suggests that the kinematic concept of fault-propagation folding is equally applicable to basement-involved, thick-skinned thrust structures.

This paper will test models of fault-propagation folding by defining and examining structural geometries from the Canadian thrust belt in Alberta. Our detailed field observations, rigorous photogrammetric profiles, and fabric analyses of four optimally-exposed folds from the Canadian thrust belt show both the complexity and diversity of fault-propagation folds. Comparisons of the structural geometries with the predictions of existing kinematic models provide tests of these models and help outline the multiple, competing processes which determine the geometries and kinematics of fault-propagation folds.

PREVIOUS STRUCTURAL MODELS

Structural explanations of asymmetric folds with variably truncated forelimbs can be roughly grouped into either sequential or simultaneous models. Willis and Willis (1934) suggested that many structures in thin-skinned thrust belts form sequentially as break-thrust folds, with flexural slip tightening regularly spaced, asymmetrical buckle folds until they lock, causing thrusts to break through their over-steepened forelimbs. Recent field (Fischer *et al.*, 1992) and experimental studies (Dixon and Liu, 1992) support this sequence of deformation in areas where early buckle folds were truncated by subsequent thrusting. The analogous 'fold-thrust' model for the basement-involved structures of the Laramide orogen (Berg, 1962; Spang *et al.*, 1985; Brown, 1988)

*Present address: Geology Department, University of California at Davis, Davis, CA 95616, U.S.A.

invokes an initial stage of basement and cover folding prior to the breakthrough of a thrust or reverse fault.

In both settings, however, irregular spacings of many asymmetrical folds with faulted forelimbs suggest that an initial stage of buckle folding may not have been an essential element of the process. In addition, many asymmetrical folds in thin-skinned thrust belts are only partially truncated by thrusts, with thrust slip transformed to fold tightening upward into the section. This indicates a period of synchronous, not sequential, faulting and folding. Similarly, in basement-involved orogens, the presence of weakly folded basement blocks under strongly folded cover strata indicates that basement faulting is often synchronous with cover folding (Erslev and Rogers, 1993).

Elliott (1976) and Williams and Chapman (1983) proposed a conceptual model for simultaneous faulting and folding where a 'tip-line' fold develops in a 'ductile bead' of material at the fault tip. Subsequent kinematic models have diverged in two directions according to their interpretation of the deformation style in the ductile bead: those invoking flexural slip during kink-band migration (Suppe and Medwedeff, 1984, 1990) and those invoking shear oblique to the beds (Dietrich and Casey, 1989; Erslev, 1991).

Suppe and Medwedeff (1984) proposed the first kinematic model for fault-propagation folding, invoking an ingenious array of kink-bands which maintained constant bed thickness during thrust propagation up a ramp (Fig. 1a). This self-similar (non-tightening) geometry predicts relatively simple relationships between the angular elements of individual structures, making it easily amenable to computer modeling. Subsequent variations of this model (Suppe and Medwedeff, 1990; Mosar and Suppe, 1992: Fig. 2a) relaxed some of the angular requirements of the original model, allowing it to be more consistent with numerous conflicting observations, including fixed anticlinal fold hinges (Fisher and Anastasio, 1994). Limited progressive tightening of folds can be accomplished by either changing bed thickness in the forelimb (Jamison, 1987, fig. 1b; Suppe and Medwedeff, 1990) or varying the thickness of the hanging wall (Mitra, 1990; Fig. 1c). Storti and Salvini (1996) attempted to explain the common occurrence of recumbent fault-propagation anticlines by adding progressive rollover kink folding to the above models.

Angular kink-band models have also been developed for basement-involved structures of the Rocky Mountains in the U.S.A. Chester and Chester (1990) modified the Suppe and Medwedeff (1984) fault-propagation fold model for faults with constant dip and compared their geometries to basement-cored structures. Narr and Suppe (1993) (Fig. 1d) approximated rounded fold surfaces using multiple, interfering kink geometries. McConnell (1994) used angular approximations to develop a model for progressive rotation in an upward-flaring kink-band emanating from a fault zone at depth.

An alternative kinematic framework is provided by models dominated by shear oblique to bedding. The sequential stretch-thrust model of Heim (1919) for alpine nappes can be envisioned as a ductile shear zone which starts wide, folding the strata, and ends narrow, faulting the strata. Ramsay and Huber (1987) showed that heterogeneous simple shear can accomplish simultaneous folding in areas of low shear strain and faulting in areas of high shear strain. But one basic problem is that the distributed shear which causes folding often occurs in front of the propagating fault zone. Dietrich and Casey (1989) recognized that the highly deformed zones in the Helvetic nappes converge toward nappe root zones, forming wedge-shaped shear zones. They superposed pure shear flattening on a tabular simple shear zone to model these deformation zones (Fig. 2a). The resulting deformation is consistent with Helvetic nappe geometries and strain, although there is no evidence of a temporal separation of the simple shear and pure shear components of deformation. In their study of two fault-propagation folds from the Iberian peninsula, Alonso

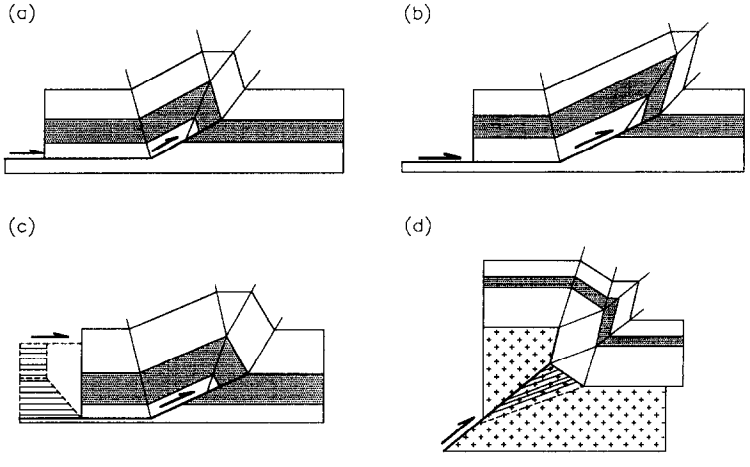

Fig. 1. Kink-band-dominated fault-propagation fold models with (a) self-similar geometries (Suppe and Medwedeff, 1984), (b) variable thickness forelimbs (Jamison, 1987), (c) layer-parallel shortening and heterogeneous shear in the hanging wall (Mitra, 1990), and (d) multiple kink-bands to approximate basement-involved structures (Narr and Suppe, 1993).

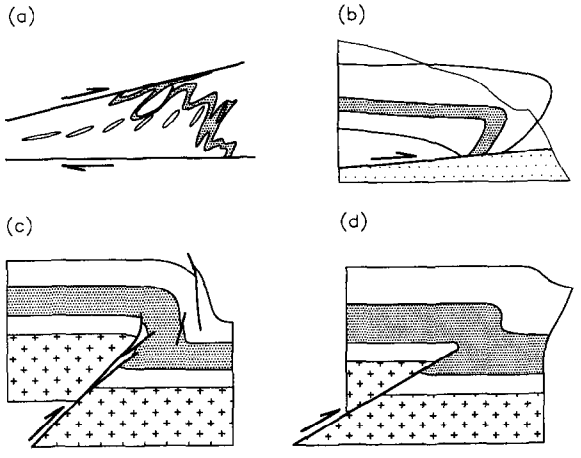

Fig. 2. Oblique shear-dominated fault-propagation fold models with (a) heterogeneous simple shear with pure shear extrusion (Dietrich and Casey, 1989), (b) angular anticlinal fold in the Pyrenees attributed to an extruding shear zone with diverging wall (Alonso and Teixell, 1992), (c) qualitative deformation in a triangular shear zone (Erslev, 1991), and (d) quantitative trishear deformation (Erslev, 1991).

and Teixell (1992) also concluded that forelimb deformation occurred in shear zones whose diverging walls caused pure shear extrusion (Fig. 2b).

Recent studies of basement-involved structures of the Rocky Mountains show that fold form, bed elongation, and fold width systematically change with structural level and displacement (Fig. 2c; Chase *et al.*, 1993; Erslev and Rogers, 1993; Evans, 1993; McConnell and Wilson, 1993; Schmidt *et al.*, 1993; McConnell, 1994). Basement fault zones flare upward into broad zones of folding. Units near the basement–cover interface tend to be tightly folded and extended adjacent to narrow zones of faulting. At higher levels, folds become more open and beds are shortened by minor thrusts and 'rabbit-ear' folds (Brown, 1988). Basement-involved fold geometries are highly variable, with rounded folds (Berg, 1976; Hennier and Spang, 1983; Stone, 1986) dominating less common angular folds (e.g. Milner Mountain anticline, Erslev and Rogers, 1993).

The complex fold geometries in basement-involved structures can be explained by viewing these folds as triangular (in profile) zones of penetrative shear which focus downward to narrow zones of simple shear at the basement–cover interface (Fig. 2c). Penetrative deformation in a triangular shear zone can be generalized using trishear, a volume-balanced incremental displacement algorithm which relaxes the simple shear requirement of parallel-sided shear zones (Fig. 2d; Erslev, 1991; Erslev and Rogers, 1993). The incremental TRISHEAR program (DOS program available free from E.A.E.) can model dip-slip faults of any angle and the resulting fold geometries given the fault angle, fault-slip rate, fault-propagation rate, apex angle of the triangular shear zone, and whether shear is uniform throughout the shear zone (homogeneous trishear) or concentrated in the center of the shear zone (heterogeneous trishear). In general, trishear predicts progressive and downward fold tightening, truncation of footwall synclines, both rounded and angular fold hinges, and complex strain patterns. These predictions contrast with those of kink-dominated models, which predict angular, commonly self-similar, geometries with migrating kink-band boundaries defining more uniformly deformed fold limbs.

FAULT-PROPAGATION FOLDS IN THE CANADIAN THRUST BELT

The geometries and deformation characteristics of four optimally exposed fault-propagation folds in the Canadian thrust belt (Fig. 3) were studied to test kinematic models of fault-propagation folding. These folds were chosen because of the quality of their exposures, with up to 1100 m of local relief, accessibility, and the lack of secondary deformation that could obscure the deformation and geometry produced by fault-propagation folding.

Regional geology and stratigraphy

The thin-skinned Canadian thrust belt extends from the Osburn fault system in Montana to the Liard River in British Columbia, 1600 km to the northwest. From west to east, the central thrust belt is divided into four physiographic provinces: the Western Ranges, Main Ranges, Front Ranges, and Foothills. Thrust faulting

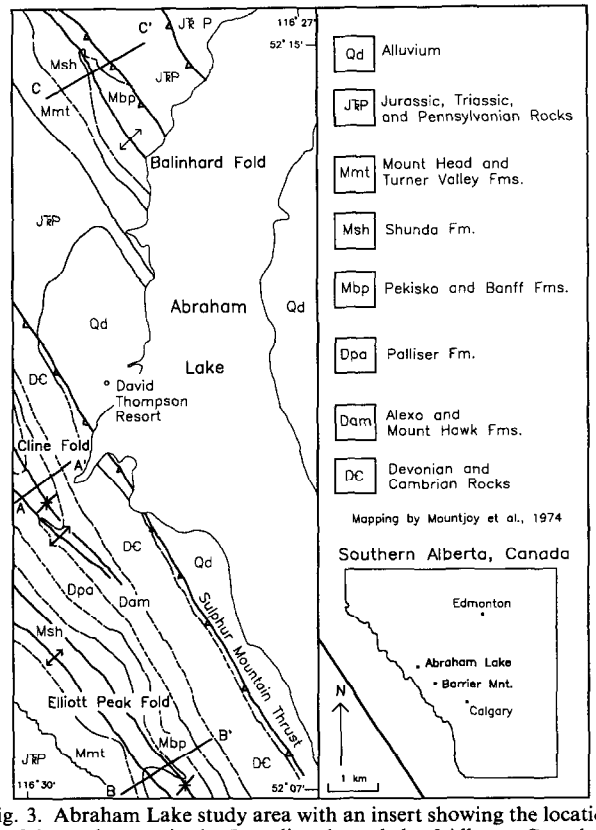

Fig. 3. Abraham Lake study area with an insert showing the locations of the study areas in the Canadian thrust belt of Alberta, Canada.

occurred during Jurassic through Oligocene time and progressed from west to east (Shaw, 1963; Dahlstrom, 1970). In the carbonate-dominated Front Ranges, detachment folds to the north near Jasper, Alberta, change southward to fault-propagation folds and then to fault-bend folds as the proportion of shaly strata decreases (McMechan and Thompson, 1989).

The Abraham Lake study area in the west half of the Whiterabbit Creek quadrangle (Mountjoy *et al.*, 1974) contains 3 well-exposed folds in the Balinhard and Sulphur Mountain thrust sheets (Fig. 3). No obvious secondary structures overprint the original fold geometries with the exception of rotation by underlying thrust imbrication. The Cline fold (Fig. 4a) is interpreted as an incipient fault-propagation fold related to a unexposed fault splay off the Sulphur Mountain Thrust. The Elliot Peak fold (Fig. 4b) shows partial truncation of strata by a thrust fault within the Sulphur Mountain thrust sheet. The Balinhard fold (Fig. 4c) is a hanging-wall anticline truncated by the Balinhard thrust, which has a slip of approximately 1 km.

The Barrier Mountain study area in the east half of the Barrier Mountain Quadrangle (Price and Mountjoy, 1971) (Fig. 3 insert) exposes the truncated hanging-wall anticline above the Clearwater thrust, a splay off the McConnell thrust with 15 km of slip. Excellent exposures of the anticlinal hinge area are provided by the valley walls of the Panther River and 3 glacial cirques.

All four folds are defined by Devonian and Mississippian carbonate rocks. The massive Palliser Formation, a grey, mottled, dolomite-rich, micritic limestone with local chert layers, is typically cut by the fault ramp responsible for the overlying fold. The lower part of the Palliser Formation consists of massive, poorly-bedded micrite and is overlain by more argillaceous and dolomitic strata in gradational contact with the Banff Formation. The Banff Formation contains finely interlayered micrite, argillaceous dolomite, and crinoidal calcarenite. Micrite layers commonly show spaced, bed-perpendicular stylolitic cleavage that probably formed during early stages of layer-parallel shortening. Axial planar, anastomosing cleavage cross-cuts the earlier stylolitic cleavage in argillaceous layers within hinge areas.

The distinctive Pekisko Formation, a light grey, crinoidal calcarenite, conformably overlies the Banff Formation. The overlying Shunda and Turner Valley formations consist of thinly- to thickly-bedded, light to dark grey, fossiliferous limestone and calcarenitic limestone. The youngest Mississippian Formation in the study areas is the Mount Head Formation which consists of dark grey limestone and argillaceous dolomite.

Methods

Detailed field measurements of over 2400 bedding, cleavage and vein attitudes were combined with photogrammetric determinations of fold shape to fully characterize the folds. Field and photogrammetric measurements of bedding orientations were used to determine fold axis orientations for plunge projections. Photogrammetric determinations of bedding orientations used three x, y, z coordinates on large bedding planes and were important in exposures where steep slopes and loose rocks made access unsafe or infeasible. Several traverses along individual beds were used to characterize fold hinge geometries. Samples were collected from all lithologies to check for strain markers, with particular emphasis on crinoidal grainstones. Fabric orientations for the Abraham Lake area are more fully discussed and tabulated in Mayborn (1993).

Special care was taken to accurately determine fold geometries in three dimensions using field photography and photogrammetry using aerial photographs. A specially calibrated Kern PG-2 plotter at the U.S.G.S. Photogrammetric Plotter Lab in Denver allowed the determination of x, y, z coordinates (± 1 m) of key marker beds from stereo pairs (Pillmore, 1989). The x, y, z coordinates were projected parallel to fold axes in order to generate plunge projections showing the true geometry of the folded exposures.

Cline fold

The Cline fold is the smallest of the three folds in the Abraham Lake area. It is exposed in the 620 m valley wall of the Cline River (Fig. 3). A photograph (Fig. 4a) and photolucida drawing (Fig. 5) of the Cline fold indicate rounded anticlinal and synclinal hinges. Eigenvector analysis of 315 bedding measurements gives a fold axis trend and plunge of 320°—19° (Fig. 5).

Two larger faults are visible from a distance in the Cline fold. The upper fault parallels bedding in the backlimb of the fold and cuts obliquely through the Pekisko Formation in the forelimb. The extra material at this ramp may be a small duplex structure. The arcuate, bed-parallel geometry of this fault suggests that it may have been present before folding. The lower fault, in the Banff Formation, cuts across bedding in the core of the fold and is bedding parallel at the synclinal hinge. This fault may be either the tip of the main fault or a minor splay. Minor faults are commonly parallel to bedding.

Poles to bedding (Fig. 5) are bimodal, suggesting a planar backlimb and forelimb. Two bedding traverses revealed variable fold geometries (Fig. 6). The top of the Palliser Formation has a very angular hinge, with the apparent dips changing from 45°SW to 50°NE in less than 10 m. A distinctive layer in the middle of the Banff Formation showed a similar change in dip over a distance of 130 m. This increased hinge zone width confirms the upward rounding geometry suggested by field photographs (Fig. 4a).

The only axial planar cleavage in the Cline structure is near the fault near the synclinal hinge. This cleavage is preferentially developed in the silty dolomitic rocks of the Banff Formation and may be due to increased deformation near the fault. Vein orientations appear fairly

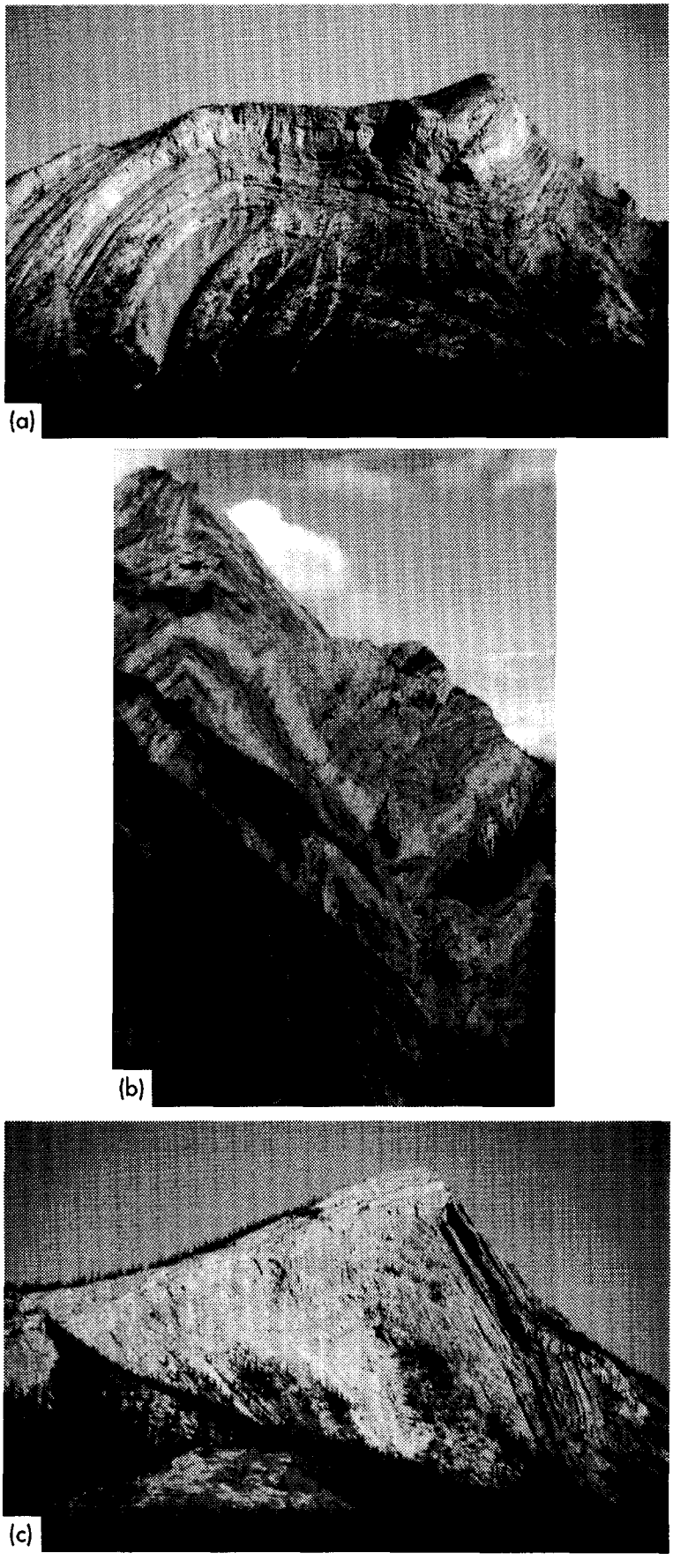

Fig. 4. Photographs of the (a) Cline, (b) Elliot Peak (Elliot 3 exposure), and (c) Balinhard folds.

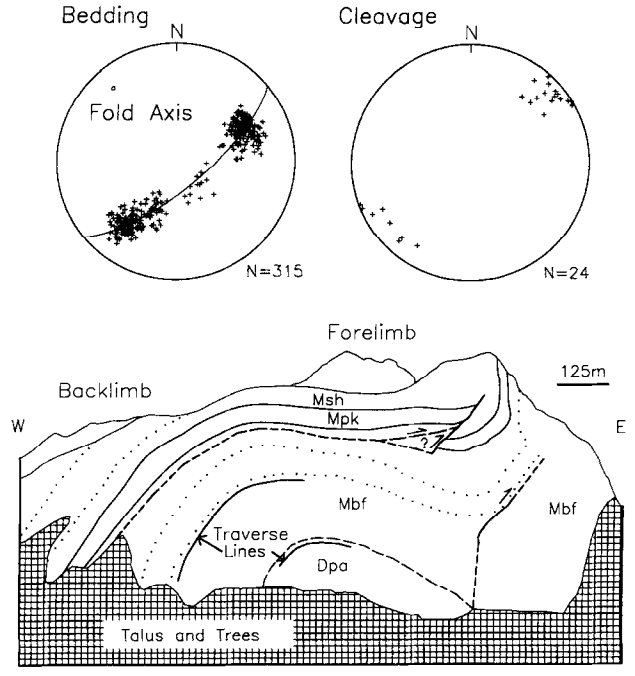

Fig. 5. Photolucida sketch of the Cline fold showing bedding traverse locations and stereonets of bedding and cleavage orientations. Scale bar is approximate due to perspective point problems. Formation key for camera lucidas, photogrammetric profiles and cross-sections: Survey Peak Fm. (COsp), Flume and Maligne Fms (Dfl), Southest Fm. (Dpx), Mt Hawk Fm. (Dmh), Alexo Fm. (Dax), Palliser Fm. (Dpa), Banff Fm. (Mbf), Pekisko Fm. (Mpk), Shunda Fm. (Msh), Turner Valley Fm. (Mtv), Mt Head Fm. (Mmh), Rocky Mountain Group (PPrm), Sulphur Mt Fm. (Trsm), Whitehorse Fm. (Trwh), Jurassic–Cretaceous Fms (JrK).

random and are restricted to the hinge and forelimb. This suggests a lack of bed-parallel shear in the backlimb because bed-parallel veins are commonly associated with flexural slip faults elsewhere in the study areas.

The down-plunge projection of the Cline fold (Fig. 7a) confirms the upward rounding fold geometry suggested by the dip traverses. In the plane perpendicular to the fold axis, the average apparent dip of the backlimb (53°SW) appears steeper than the dip in the photograph (Fig. 4a) due to projection corrections for the inclined fold axis.

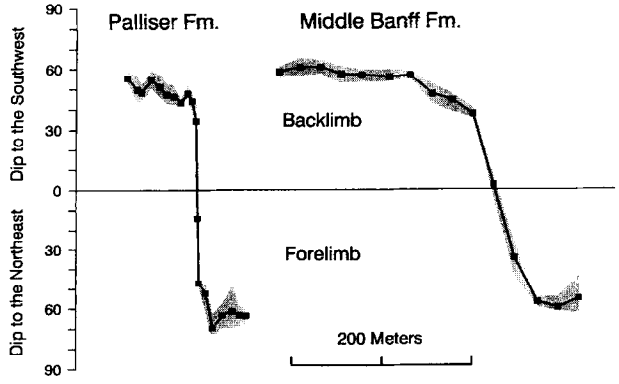

Fig. 6. Apparent dip averages (solid lines) and ranges (shaded areas) of bedding orientations collected on bed-parallel traverses in the Banff and Palliser formations (see Fig. 5 for locations). Apparent dips are calculated for the plane perpendicular to the fold axis.

Elliot Peak fold

The Elliot Peak fold (Figs 4b, 7b & c & 8) is a spectacular fault-propagation fold where the Palliser Formation is cut by a thrust which dies in the folded Banff Formation. The Elliot 1 exposure has roughly 300 m of relief and is the least dramatic of the 3 Elliot exposures because much of the forelimb has been eroded away. A bed-parallel thrust fault in the backlimb partially truncates the crest of the angular anticline. The bimodal bedding orientations of the Shunda Formation give a fold axis orientation of 332°—12° (Fig. 8), with a planar forelimb and a more variable backlimb whose dips range from 85° to 45°. Axial planar cleavage and veins are concentrated in the hinge. The near-vertical cleavage orientations do not change significantly from the hinge to the forelimb. Thin sections show cleavage zones truncating bioclasts, indicating pressure solution.

The plunge projection of the Elliot 1 exposure does not supply much information because of the limited exposure of the forelimb. The hinge is angular and the forelimb is planar. The backlimb is slightly undulatory, confirming the bedding data in Fig. 8, and has an apparent dip of 59°SW. Thickness changes in the forelimb cannot be determined because the layers traced in the backlimb are not the same layers traced in the forelimb.

The Elliot 2 exposure is on the 600 m high, northwest face of Elliot Peak (Fig. 3). Oblique and vertical aerial photographs provided the only data for this part of the fold (Fig. 7b). The hinge is angular and is rounded only at the lowest exposures. In the core of the fold, a backthrust in the forelimb turns slightly as it enters the core and then dies out. In addition, a small thrust in the backlimb cuts across bedding. The extra strata brought into the fold hinge by these faults contribute to the angularity of the hinge by filling the space between the angular limbs.

The fold axis (317°—6°) at the Elliot 2 exposure was calculated with photogrammetric determinations of bedding attitudes. Beds in the core of the anticline curve through the hinge and are truncated by the backthrust. The upper beds form an angular hinge. The backlimb dips roughly 70°SW and the forelimb dips 55°NE. The forelimb does not appear to be thickened or thinned relative to the backlimb.

The Elliot 3 exposure, with 1100 m of relief over a map distance of 1850 m, gives the most complete profile through a fault-propagation fold in the area (Figs 4b & 7c). A photolucida (Figs 8) of a photograph taken from an overlook next to the exposed thrust in the Palliser Formation shows the complex geometry and deformation in the fold. The lowest beds in the anticline form angular hinges, with more rounded hinges at intermediate levels. At higher levels, a backthrust on the forelimb cuts the angular hinge region. Several other backthrusts in the forelimb are mostly parallel to bedding except where they form small ramp anticlines. The upper backthrust appears to truncate the fold created by the lower backthrust. These faults appear to originate near

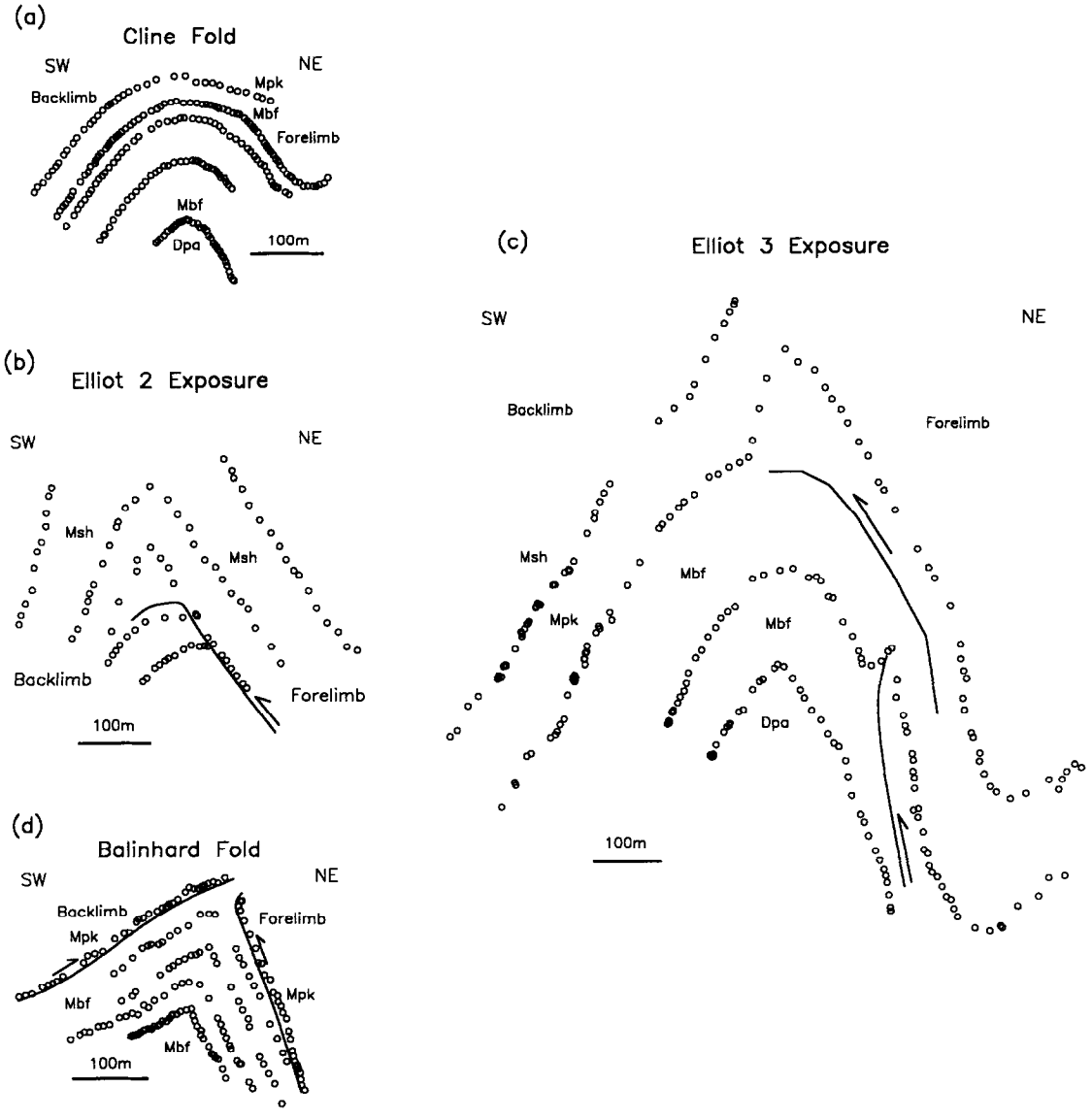

Fig. 7. Plunge projections of photogrammetric data defining prominent bedding horizons in the (a) Cline, (b, c) Elliot Peak, and (d) Balinhard folds. Formation key in Fig. 5.

the rounded, synclinal hinge which is complicated by many smaller-scale faults and folds.

The plunge projection (Fig. 7c) clearly shows that the anticlinal hinge geometry changes from angular to rounded and then back to angular with height in the fold. The angularity of the upper hinge is caused by the upper backthrust which duplicates strata in the hinge region. The upper portion of the forelimb appears to be slightly thickened (3%) relative to the more planar backlimb. The lower portion of the forelimb is thinned by approximately 20%.

In summary, the Elliot Peak fold is a tight fold with a single axial plane. Both angular and rounded anticlinal hinges occur, with angular hinges commonly associated with thrusts and backthrusts which transport extra strata into the hinge region. The synclinal hinge in the Elliot 3 exposure is rounded and complicated by intermediate scale folding and faulting.

Balinhard fold

The Balinhard fold (Figs 4c, 7d & 9) is exposed in a 600 m high mountainside. It is probably the most evolved of the three folds in the Abraham Lake area because Balinhard thrust splays cut the forelimb of the fold. The two smaller faults (Fig. 9) are mostly bedding-parallel except where they cut bedding at the anticlinal hinge.

Bimodal bedding attitudes indicate an angular anticlinal hinge oriented 146°—12° (Fig. 9). Backlimb bedding dips change from 31°SW near the hinge to 46°SW farther away from the hinge. Forelimb bedding dips uniformly 75°NE except in the lowermost, backthrust Pekisko Formation where beds range from 80°NE to 80°SW (overturned). A bedding traverse within the Banff Formation (Fig. 10) shows a narrow hinge zone less than 40 m wide. The backlimb dip shallows immediately adjacent to the hinge, possibly due to a hidden backthrust

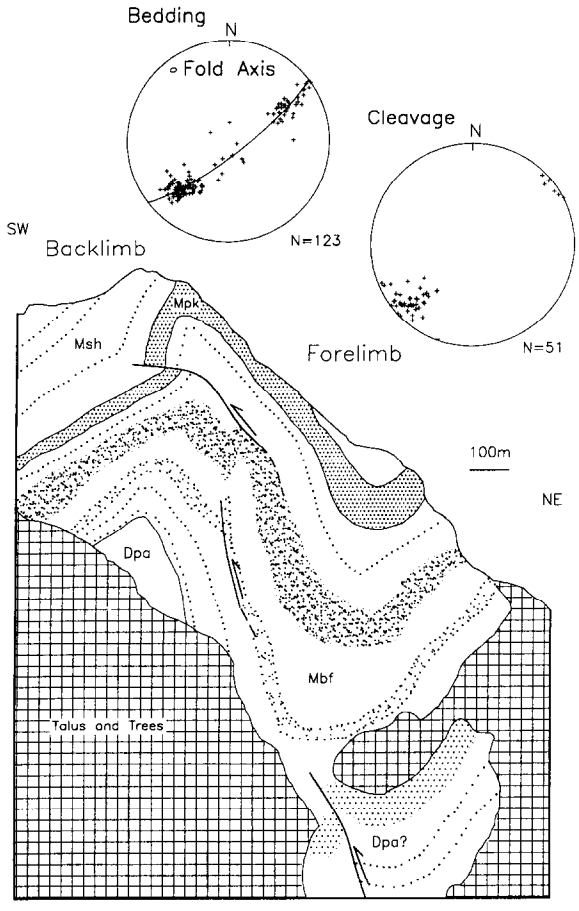

Fig. 8. Photolucida sketch of the Elliot 3 exposure and stereonets of bedding and cleavage orientations from the Elliot 1 exposure. Scale bar is approximate due to perspective point problems. Formation key in Fig. 5.

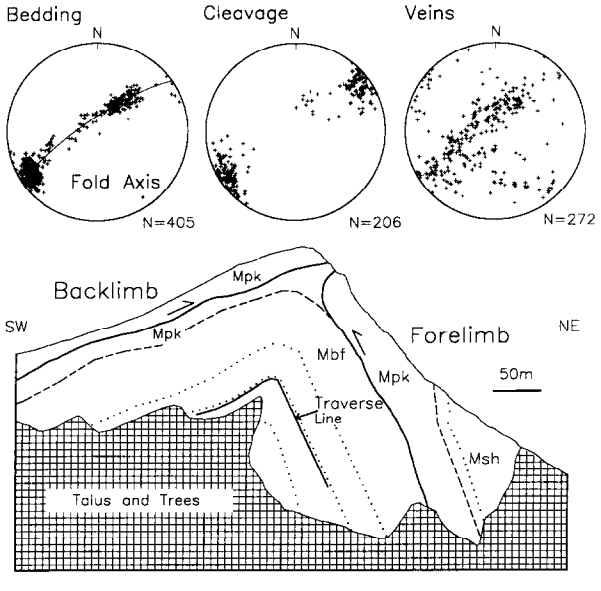

Fig. 9. Photolucida sketch of the Balinhard fold showing the bedding traverse location and stereonets of bedding, cleavage and vein orientations. Formation key in Fig. 5.

adding material to the hinge area similar to the Elliot 2 and Elliot 3 exposures.

The Balinhard fold contained the most abundant cleavage of any of the folds studied, with both early layer-perpendicular and later axial planar cleavage (Fig. 9). The backlimb and hinge areas are dominated by vertical cleavage, with greatest abundance of cleavage at the hinge where it is axial planar to the fold. Forelimb cleavage is more parallel to bedding and is preferentially developed in the silty dolomite layers of the Banff Formation. Veins in the Balinhard structure are concentrated in the forelimb (Fig. 9) where they are commonly bedding parallel and associated with slip surfaces.

The plunge projection for the Balinhard fold (Fig. 7d) reveals uniformly angular fold geometries. There is some rounding in the anticlinal hinges below the faults, but it becomes angular again above the faults. The interlimb angle for the faulted strata is 71° and there is no appreciable thickness difference between the forelimb and the backlimb.

Fabric analysis of the Abraham Lake structures

One surprise from the photogrammetric analyses is that forelimb strata show minimal evidence of penetrative deformation. The only exposure in the Abraham Lake area which showed variations in thickness was the Elliot 3 exposure, where up to 20% thinning was seen on the lower forelimb relative to the backlimb. This value should be treated with suspicion, however, because the fold axis for the plunge projection was based on relatively few photogrammetric measurements of bedding. A different fold axis for this part of the fold or a conical geometry could easily explain this apparent thickness variation.

Field observations of what appeared to be undeformed fossils on the forelimbs of the folds further suggest low penetrative strain. To test this possibility, crinoidal grainstones were collected for strain analysis. Twenty thin sections were cut in the plane of the cross-sections

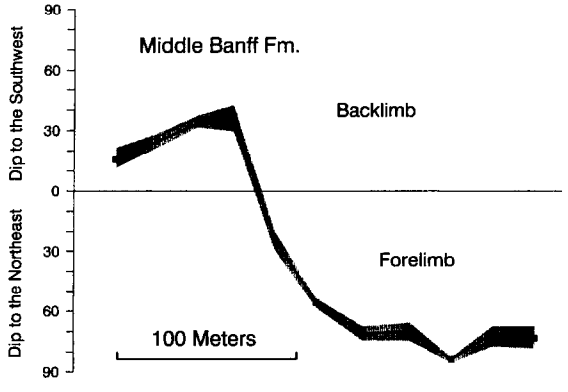

Fig. 10. Apparent dip averages (solid lines) and ranges (shaded areas) of bedding orientations collected on bed-parallel traverses in the Banff Formation (see Fig. 9 for locations). Apparent dips are calculated for the plane perpendicular to the fold axis.

and examined for signs of deformation. Poor packing in many samples made center-to-center strain analysis impractical, so object ellipticities of crinoidal bioclasts were determined with the mean object ellipse method (Erslev and Ge, 1990). Initial ellipticities were evaluated for three orthogonal planes in one apparently undeformed backlimb sample. The low fabric ellipticities of this sample (X/Y: 1.14, 1.13, 1.14) suggests low regional fabric anisotropies probably due to both depositional and deformation processes.

The fabric data in the plane of the cross-sections for 3 Abraham Lake localities are plotted in Fig. 11. Details of the treatment are given in Mayborn (1993) and are not reproduced here because the results showed that the fabric anisotropies ranged from 1.03 to 1.28, very close to the regional fabric values. In addition, there was little consistency or reproducibility relative to fold position, showing that penetrative strains, as measured by crinoid bioclasts, were probably very low in these rocks.

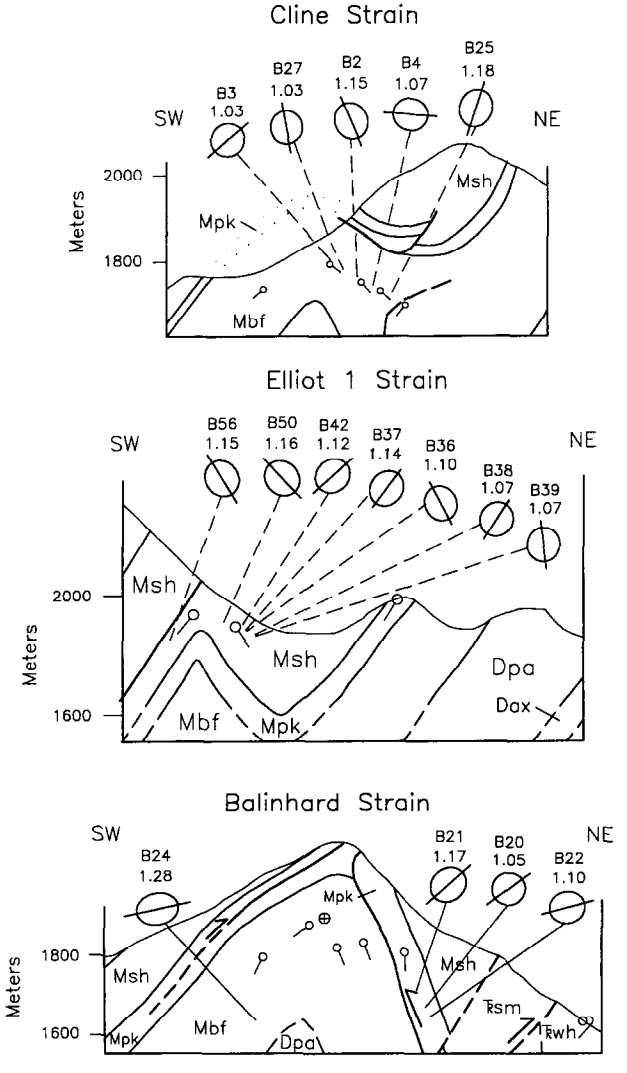

Fig. 11. Fabric ellipses derived from mean object ellipse calculations of crinoidal grainstones plotted on profiles of the Abraham Lake structures. Formation key in Fig. 5.

Barrier Mountain fold

Due to their varying degree of development, the fold geometries from the Abraham Lake area (Fig. 12) can be viewed either as the progressive evolution of a single structure or as normal variations in geometry due to local factors. The trade of space for time suggested by the evolutionary hypothesis is a traditional approach in structural geology and requires that local conditions in the structures remained the same, with the only difference being the amount of slip represented in the individual structures. The cross-sections in Fig. 12 show anticlinal interlimb angles tightening from the Cline (74° to 109°) to the Elliot Peak (45° to 59°) folds, consistent with non-self-similar fold models. But the fact that the Balinhard fold has a larger interlimb angle (72° to 84°) than the Elliot Peak fold suggests at least a component of local variability because it is unlikely that the interlimb angles would get larger with increased displacement.

The diversity of fold angularity, from the rounded fold surfaces in the Cline fold to the wholly angular geometries at the Balinhard fold, is difficult to understand. One possibility is that rounded folds (e.g. Cline fold) become more angular with time, perhaps to accommodate more shortening in the structure. This would require the straightening of the forelimb during folding, for which we see no evidence. Alternatively, fold curvature could be due to local effects, such as the position of major backthrusts and the local dominance of different modes of folding. To test these possibilities, multiple exposures of a truncated fault-propagation fold at Barrier Mountain, Alberta (Fig. 13), were studied to see whether variations in fold geometry, like the occurrence of rounded and angular hinges, are due to local effects or progressive stages of deformation.

The Barrier Mountain fold north of the Panther River represents an even further evolved structure, with Price and Mountjoy (1971) interpreting approximately 15 km of slip on the underlying Clearwater thrust. This study examined exposures of the fold's hinge area and forelimb north of the Panther River in the northeastern side of Barrier Mountain. Bedding orientations from the hinge and forelimb of the fold (Fig. 13) are scattered in a great circle about an average fold axis oriented 322°—04°. Fold axes for individual exposures give similar values, indicating a common fold axis for all exposures. The forelimb of the fold varies from highly overturned (commonly around 45°SW) to near vertical (Figs 14 & 15). Areas of high-angle dips in the forelimb show relatively little bedding plane distortion but the hinge areas are intensely contorted. Axial planar cleavage is largely limited to the argillaceous Banff Formation in the anticlinal hinge. Veins are most common in the anticlinal hinge and forelimb where they parallel backthrust orientations or formed complex arrays of gash fractures.

Fold form changes dramatically along strike. The southern-most profile, exposed in the Panther River canyon (Figs 14a & 15c), shows a highly angular fold,

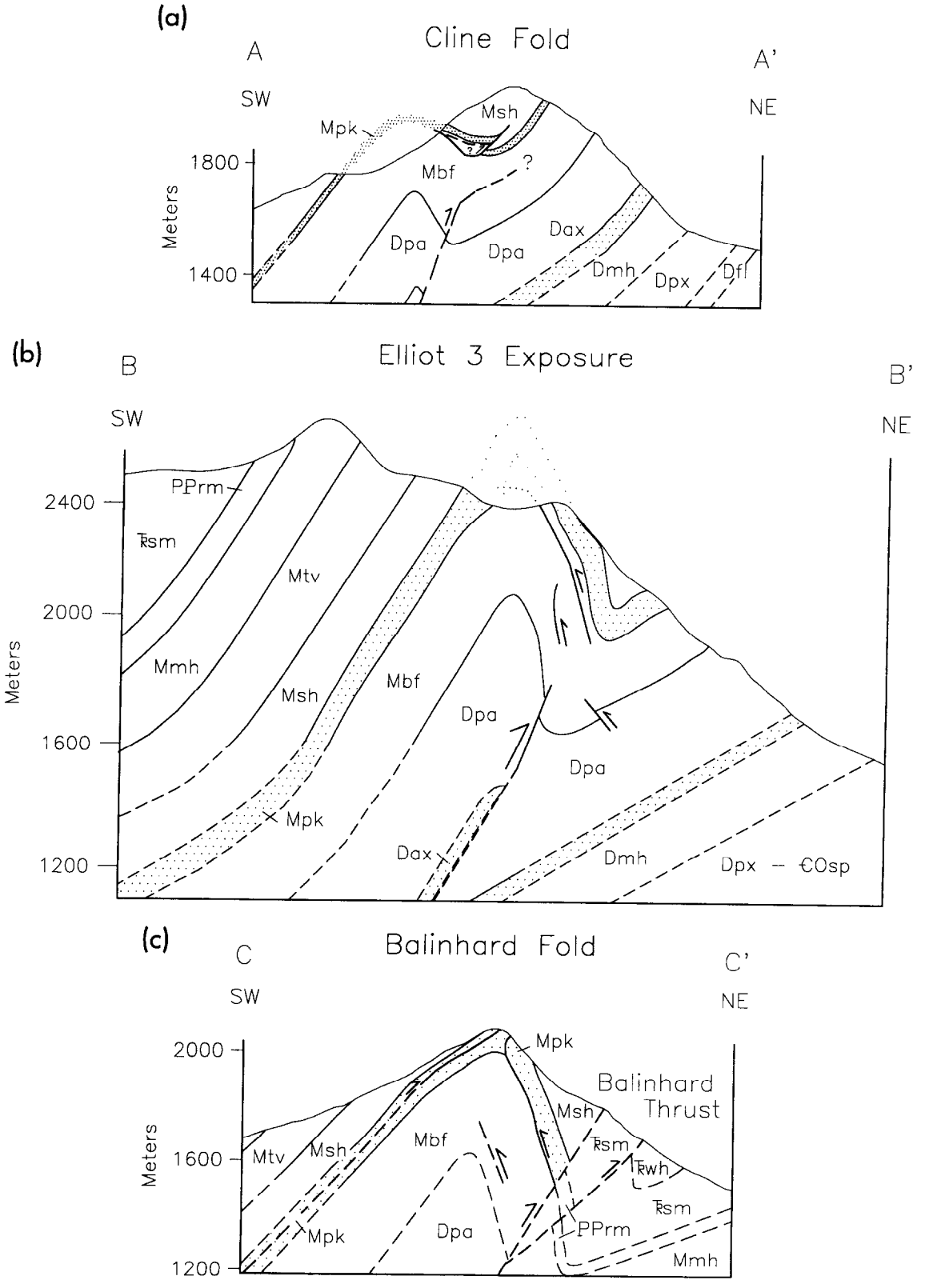

Fig. 12. Cross-sections through the (a) Cline, (b) Elliot Peak, and (c) Balinhard fault-propagation folds. Formation key in Fig. 5.

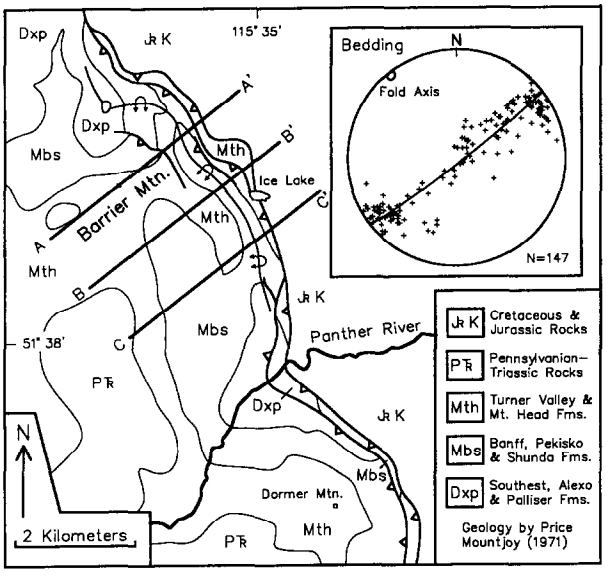

Fig. 13. Location map for the Barrier Mountain study area with an inset stereonet of bedding orientations measured along the northeast side of Barrier Mountain.

with hinge distortion by major bedding-parallel forethrusts and backthrusts. Within the fold hinge where the strata rolls over, many bedding parallel surfaces on both limbs abruptly ramp upward through bedding, revealing substantial layer-parallel slip directed toward the anticlinal hinge. Further north, however, the fold is more recumbent and much more rounded (Figs 14b & 15b). Extreme contortion in the Banff Formation within the fold hinge area appears to be related to rotated backthrusts in the forelimb. These folds are cut by planar faults emanating from bedding planes in the backlimb. Even further north, the backlimb of the thrust sheet forms a box-like geometry (Fig. 15a), possibly due to fault-bend folding after fault-propagation folding. The anticlinal fold suddenly becomes angular and the forelimb is again nearly planar and close to vertical.

Photogrammetry was limited to the southern area due to the availability and angles of aerial photographs (Fig. 16). The Panther River exposure shows a rounded and recumbent fold geometry in the upper Palliser. Above the Banff Formation, the Pekisko Formation is highly angular, with extra material transported on forethrusts

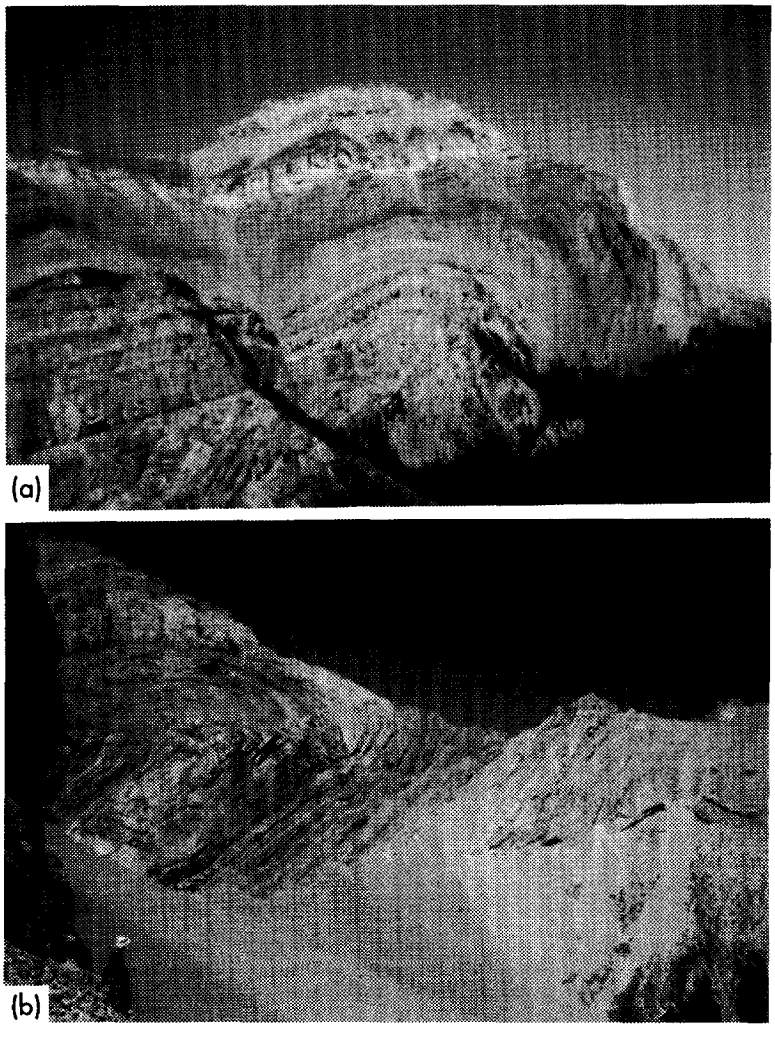

Fig. 14. Photographs of the (a) Panther River and (b) Ice Lake exposures of the Barrier Mountain fold.

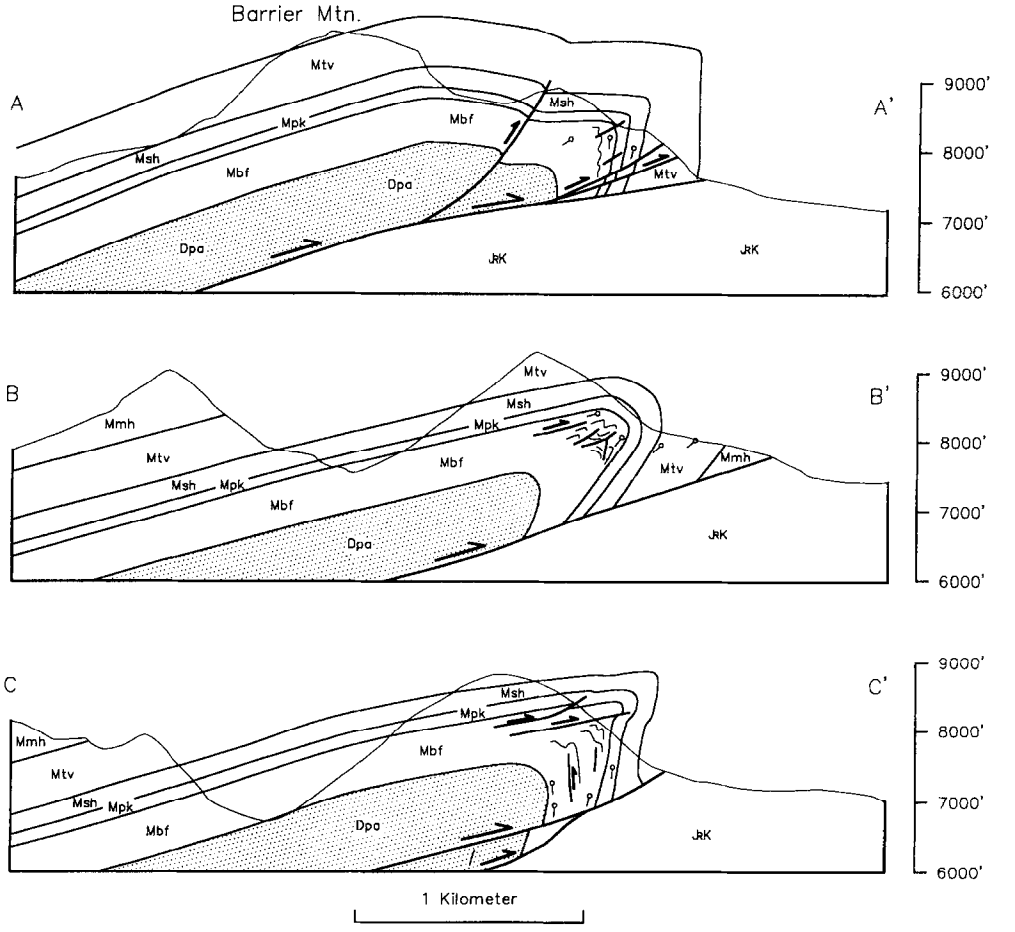

Fig. 15. Northeast-trending cross-sections through the Barrier Mountain fold showing the variations in fold geometry along strike. Formation key and lines of section in Fig. 13.

and backthrusts filling in the hinge area. Just to the north, however, the Pekisko Formation forms a rounded, recumbent fold consistent with field observations at Ice Lake cirque.

Thin sections from the Barrier Mountain fold confirm the general lack of penetrative deformation in limestones from the forelimb and hinge. Of 27 thin sections, only 4 show measurable deformation: three micritic samples of Palliser Formation and one crinoidal grainstone from the Turner Valley Formation. The Palliser samples were collected in the arcuate hinge and forelimb of the Panther River and all showed short pressure shadows on pyrite cubes indicating minor extension parallel to cleavage. These cleavage-parallel elongations in the more tightly folded Palliser Formation do suggest penetrative deformation but the irregular distribution of pyrite made a systematic study impractical. Of the crinoidal samples sectioned, only one shows clear penetrative strain, with elongation in the dip-direction of the Clearwater thrust. All other samples, including one taken 5 m from the above mentioned sample, show no clear evidence of measurable strain anisotropy. This indicates minimal penetrative strain in the forelimb, with localized zones of higher strain whose scale would necessitate much more detailed sampling for an adequate definition of the strain. Our unsuccessful attempts to measure penetrative strains in the planar forelimb and angular hinge areas of these fault-propagation folds confirms the dominance of flexural slip deformation observed in the field and deduced from the lack of significant changes in unit thicknesses.

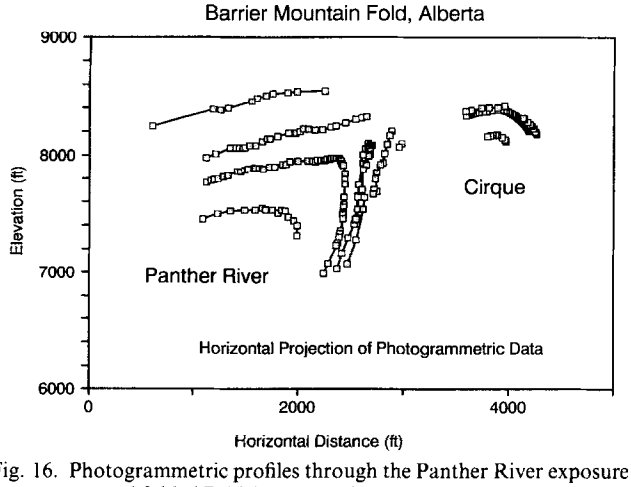

Fig. 16. Photogrammetric profiles through the Panther River exposure and folded Pekisko Formation near Ice Lake.

DISCUSSION

Fault-propagation folds from the Canadian thrust belt show a variety of geometries ranging from recumbent, curved folds to more open, highly-angular folds. In all the cases studied here, anticlinal hinges define single planes which diverge upward from zones of faulting and tight folding in the Palliser Formation. Anticlinal hinge areas commonly show highly contorted beds due to fold tightening of the hinge and transport of extra strata into the hinge by bedding-parallel thrusts and backthrusts. Comparison of the intense deformation in anticlinal hinges with the minimal deformation in adjacent forelimbs indicates that anticlinal hinges were fixed during folding because it is difficult to imagine a process which could unfold the contorted hinge areas into planar forelimbs.

Cross-sections from the Abraham Lake area (Fig. 12) generally show a progressive tightening of the unfaulted strata, from the rounded Cline fold, with interlimb anticlinal angles of 74° to 109°, to the Elliott Peak fold with interlimb angles of 45° to 59°. Interlimb angles for fault-truncated strata also vary, from 72° to 84° in the Balinhard fold to 27° to 70° in the Barrier Mountain fold. The variability of fold geometries along strike in the Barrier Mountain fold shows that these geometries are not simply a function of fault angle, fault slip and/or lithologic controls as postulated by some models of fault-propagation folding.

Internal deformation in the folds is dominated by flexural slip on bedding planes, with thrust motions directed toward anticlinal hinges. Photogrammetric measurements show minimal consistent differences between forelimb and backlimb thicknesses. Bed attenuation is relatively rare, with local thickening common in anticlinal hinges due to thrust duplication of strata in the hinge areas. Penetrative strain is minimal and mostly limited to cleavage-related flattening in fold hinges and localized simple shear zones related to thrust propagation and flexural shear on fold limbs. The prevalence of bedding-parallel slip indicates that overall distortions may be quite large, particularly in the forelimb and hinge areas, but the scale of strain heterogeneity would have necessitated much more detailed sampling in order to quantify these distortions.

Comparisons of the fold geometries with previous kink-band and oblique shear models (Figs 1 & 2) show that no individual model can adequately explain the kinematic development of these folds. Some arcuate fold surfaces can be explained by an initial stage of buckle folding, but the curved, recumbent surfaces of the Barrier Mountain fold indicates that curved fold surfaces are also generated during fault-propagation folding. Oblique shear models (Fig. 2) such as trishear can explain the arcuate anticlinal (e.g. Panther River exposure of the Barrier Mountain fold) and synclinal (Cline and Elliot 3 exposures) fold surfaces in the massive Upper Palliser Formation. But they are contradicted at higher structural levels by the highly angular fold surfaces and minimal strains recorded in the forelimbs of these structures. An inherent problem with applying the trishear model to structures involving well-bedded sedimentary strata is the inability of the trishear algorithm to model the bedding anisotropy responsible for flexural slip folding.

In any case, the narrow zones of faulting at depth need to be linked with the angular folding in the upper levels of the structures. We suggest that distributed shear in a triangular shear zone can bridge this gap, with rounded fold surfaces occurring where massive units deform by oblique shear, and with angular fold surfaces occurring where better-layered units deform by flexural slip.

The dominance of angular fold surfaces at higher levels in the folds suggests the application of kink-band fault-propagation fold models (Fig. 1). But these models predict box-like anticlines with multiple, migrating hinges in unfaulted strata. These geometries are inconsistent with the single, fixed anticlinal fold hinges in the unfaulted strata of the Cline and Elliot Peak folds as well as other examples from Williams and Chapman (1983) and Fisher and Anastasio (1994). Self-similar fold development, where fold shapes and angles remain the same as kink-band migration creates a bigger structure, is contradicted by the variability of forelimb orientations and evidence for fold tightening with increasing structural displacement. In addition, the curvature of many fold surfaces is not predicted by kink-band models.

One alternative to explain the angular folds is to model them with progressive kink folding by flexural slip (Fig. 17). In this model, analogous to the fixed-hinge chevron folding of Stewart and Alvarez (1991), fixed fold hinges cause progressive limb rotation during folding until the limbs lock, requiring thrusting either through the forelimb or along a fold hinge to accommodate additional deformation. This model requires flexural slip throughout the section, with synthetic thrusting on backlimb bedding planes and antithetic backthrusting on forelimb bedding planes. In addition, synthetic thrusting forward of the synclinal axis is generated by the progressive (clockwise in Fig. 17) rotation of the synclinal hinge lines. As a result, progressive kink folding provides a mechanism for transmitting regional layer-parallel shear through folds in the direction of general tectonic transport.

The combination of triangular shear zone folding near propagating thrusts with progressive kink folding at higher levels is illustrated in Fig. 18. Figure 18(b) was generated by balancing a generalized version of the Elliot 3 cross-section (Fig. 12b) and rotating it so that footwall bedding is horizontal. The angular anticlinal fold geometry in the upper strata combined with our interpretation of fixed anticlinal hinges requires flexural slip and/or flexural shear to transport material into the anticlinal hinge area, consistent with our field observations. A delicate balance between the competing fold mechanisms appears to govern the location of the transition from triangular shear zone folding to progressive kink folding. Variability in the stratigraphic level of

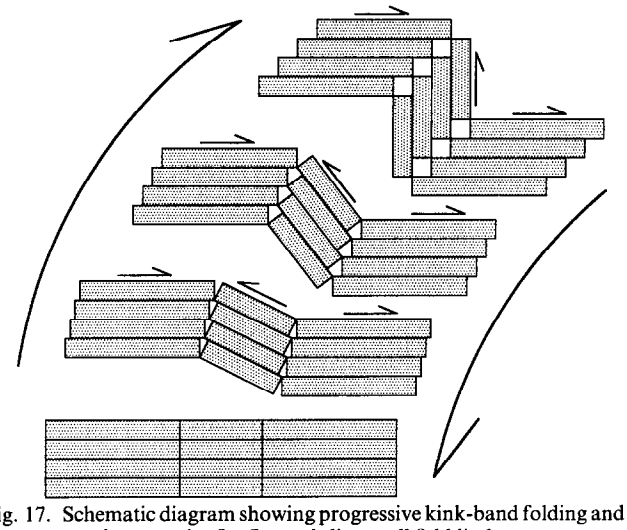

Fig. 17. Schematic diagram showing progressive kink-band folding and the necessity for flexural slip on all fold limbs.

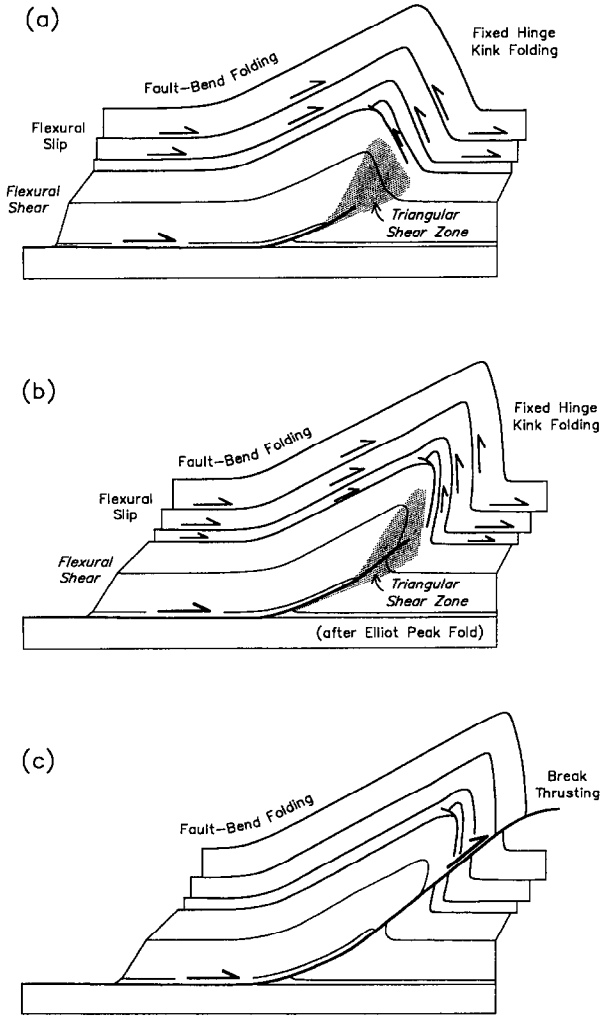

Fig. 18. Balanced, multi-mode fault-propagation fold model for thin-skinned thrust belts based on the Elliot 3 exposure (b), retrodeformed to an earlier configuration (a), and truncated by a subsequent break-thrust (c).

this transition within individual structures can explain why the Pekisko Formation in the Barrier Mountain fold forms both angular and rounded fold surfaces.

An increment of retrodeformation applied to the Elliot Peak section (Fig. 18b) gives a possible earlier stage of deformation (Fig. 18a), which is similar to many detachment fold geometries (Homza and Wallace, 1997). Further progressive kink folding of the Elliot Peak structure, as modeled in Fig. 18(b), would probably tighten the folded layers uniformly until they locked and broke, resulting in break-thrust folding (Fig. 18c). Thus, different modes of fault-propagation folding should result in different fault-propagation rates. In triangular shear zone portions of folds, the master thrust may propagate proportional to fault slip. In the areas of progressive kink folding, where folds tighten uniformly and lock, the master thrust may propagate very rapidly as a break thrust.

Progressive kink folding requires synthetic flexural slip in the backlimb and thus the presence or absence of regional flexural slip may control its development. In the case of the curved fold surfaces in the Cline fold, if folding occurred with relatively little backlimb flexural slip (as indicated by field observations), then progressive kink folding may have been inhibited, resulting in a more arcuate fold geometry. Similarly, the general lack of regional bed-parallel slip in the basement-involved folds of the Laramide Orogen (U.S.A.) may have suppressed progressive kink folding in the many examples of basement-cored folds with arcuate fold hinges. Thus, the presence (in many thin-skinned structures) or absence (in many thick-skinned structures) of regional bed-parallel slip may be responsible for some of the differences in fault-propagation fold geometries from these orogens.

These two modes of fault-propagation folding, triangular shear zone folding and progressive kink folding, are competitive processes, with their development dependent on the degree of bedding anisotropy and presence of regional bedding-parallel slip. In addition, buckling both before and during fault-propagation folding undoubtedly has important contributions to fold geometries. Additional fold mechanisms generating the self-similar kink-band geometries of Suppe and Medwedeff (1990) may also occur, perhaps at shallower levels in the crust, but no evidence for collaborative geometries was seen in this study. For the areas studied here, self-similar kink-band models are useful as reproducible approximations that allow regional extrapolations. However, detailed analyses of reservoir and fracture geometries in asymmetric thrust-cored folds will need to consider the combination of triangular shear zone folding and progressive kink folding which occur in fault-propagation folds of the Canadian thrust belt.

Acknowledgements—Reviews, comments and suggestions by David Anastasio, Peter Hennings, Christopher Hedlund, and G. J. Rait were greatly appreciated. Steve Schultz assisted with field work and petrographic analyses. We are indebted to Henry Charlesworth and

Philip Simony for suggesting the field areas in the Canadian Rockies. Charles Pillmore and Jim Messerich at the U.S.G.S. Photogrammetric Plotter Lab in Denver provided access to and help with photogrammetric equipment. This research was supported by the donors of the Petroleum Research Fund, administered by the Petroleum Research Fund, and N.S.F. grant EAR-9304547. Additional funding was provided by grants from ARCO, Chevron and the Geological Society of America.

REFERENCES

Alonso, J. L. and Teixell, A. (1992) Forelimb deformation in some natural examples of fault-propagation folds. In *Thrust Tectonics*, ed. K. R. McClay, Chapman and Hall, London, 175–180.

Berg, R. R. (1962) Mountain flank thrusting in Rocky Mountain foreland, Wyoming and Colorado. *Bulletin of the American Association of Petroleum Geologists* **46**, 2019–2032.

Berg, R. R. (1976) Deformation of Mesozoic shales at Hamilton Dome, Bighorn basin, Wyoming. *Bulletin of the American Association of Petroleum Geologists* **60**, 1425–1433.

Brown, W. G. (1988) Deformation style of Laramide uplifts in the Wyoming foreland. In *Interaction of the Rocky Mountain Foreland and the Cordilleran Thrust Belt*, eds C. J. Schmidt and W. J. Perry, Jr, Geological Society of America Memoir **171**, 53–64.

Chase, R. B., Genovese, P. W. and Schmidt, C. J. (1993) The influence of Precambrian rock compositions and fabrics on the development of Rocky Mountain foreland folds. In *Basement–Cover Kinematics of Laramide Foreland Uplifts*, eds C. J. Schmidt, R. B. Chase and E. A. Erslev, Geological Society of America Special Paper **280**, 45–72.

Chester, J. S. and Chester, F. M. (1990) Fault-propagation folds above thrusts with constant dip. *Journal of Structural Geology* **12**, 903–910.

Dahlstrom, C. D. A. (1970) Structural geology in the eastern margin of the Canadian Rocky Mountains. *Bulletin of the Canadian Petroleum Geologists* **46**, 332–406.

Dietrich, D. and Casey, M. (1989) A new model for the Helvetic nappes. In *Alpine Tectonics*, eds M. P. Coward, D. Dietrich and R. G. Park, Geological Society Special Publication **45**, 47–63.

Dixon, J. M. and Liu, S. (1992) Centrifuge modelling of the propagation of thrust faults. In *Thrust Tectonics*, ed. K. R. McClay, pp. 53–70. Chapman and Hall, London.

Elliott, D. W. (1976) The energy balance and deformation mechanisms of thrust sheets. *Philosophical Transactions of the Royal Society of London* **A283**, 289–312.

Erslev, E. A. (1991) Trishear fault-propagation folding. *Geology* **19**, 617–620.

Erslev, E. A. and Ge, H. (1990) Least-squares center-to-center and mean object ellipse fabric analysis. *Journal of Structural Geology* **12**, 1047–1059.

Erslev, E. A. and Rogers, J. L. (1993) Basement-cover geometry of Laramide fault-propagation folds. In *Laramide Basement Deformation in the Rocky Mountain Foreland of the Western United States*, eds C. J. Schmidt, R. B. Chase and E. A. Erslev, Geological Society of America Special Paper **280**, 125–146.

Evans, J. P. (1993) Deformation mechanisms and kinematics of a crystalline-cored thrust sheet: the Washakie thrust system, Wyoming. In *Laramide Basement Deformation in the Rocky Mountain Foreland of the Western United States*, eds C. J. Schmidt, R. B. Chase and E. A. Erslev, Geological Society of America Special Paper **280**, 147–162.

Fischer, M. P., Woodward, N. B. and Mitchell, M. M. (1992) The kinematics of break-thrust folds. *Journal of Structural Geology* **16**, 451–460.

Fisher, D. M. and Anastasio, D. J. (1994) Kinematic analysis of a large-scale leading edge fold, Lost River Range, Idaho. *Journal of Structural Geology* **16**, 337–354.

Heim, A. (1919) *Geologie der Schweiz*. Tauchnitz, Leipzig.

Hennier, J. and Spang, J. H. (1983) Mechanisms for deformation of sedimentary strata at Sheep Mountain anticline, Bighorn Basin, Wyoming. *Wyoming Geological Association Guidebook* **34**, 96–111.

Homza, T. X. and Wallace, W. K. (1997) Detachment folds with fixed hinges and variable detachment depth, northeastern Brooks Range, Alaska. *Journal of Structural Geology* **19**, 337–354.

Jamison, W. R. (1987) Geometric analysis of fold development in overthrust terranes. *Journal of Structural Geology* **9**, 207–220.

Mayborn, K. R. (1993) Geometry and deformation of three fault-propagation folds in the Front range of the Canadian thrust belt. Unpublished M.Sc. thesis, Colorado State University, Fort Collins, Colorado.

McConnell, D. A. (1994) Fixed-hinge, basement-involved fault-propagation folds, Wyoming. *Bulletin of the Geological Society of America* **106**, 1583–1593.

McConnell, D. A. and Wilson, T. G. (1993) Linkage between deformation of basement rocks and sedimentary rocks in basement-involved folds. In *Basement–Cover Kinematics of Laramide Foreland Uplifts*, eds C. J. Schmidt, R. Chase and E. A. Erslev, Geological Society of America Special Paper **280**, 319–335.

McMechan, M. E. and Thompson, R. I. (1989) Structural style and history of the Rocky Mountain fold and thrust belt. In *Western Canada Sedimentary Basin*, ed. B. D. Ricketts. Canadian Society of Petroleum Geologists, pp. 47–72.

Mitra, S. (1990) Fault-propagation folds: Geometry, kinematic evolution, and hydrocarbon traps. *Bulletin of the American Association of Petroleum Geologists* **74**, 921–945.

Mosar, J. and Suppe, J. (1992) Role of shear in fault-propagation folding. In *Thrust Tectonics*, ed. K. R. McClay, pp. 123–132. Chapman and Hall, London.

Mountjoy, E. W., Price, R. A., Aitken, J. D. and Cook, D. G. (1974) Geologic map of Whiterabbit Creek (west half), Alberta. Geological Survey of Canada map 1389A.

Narr, W. and Suppe, J. (1993) Kinematics of basement-involved compressive structures. *American Journal of Science* **294**, 302–360.

Pillmore, C. L. (1989) Geological photogrammetry in the U.S. Geological Survey. *Photogrammetric Engineering and Remote Sensing* **55**, 1185–1189.

Price, R. A. and Mountjoy, E. W. (1971) Geology Barrier Mountain (east half). Geological Survey of Canada map 1273A.

Ramsay, J. G. and Huber, M. I. (1987) *The Techniques of Modern Structural Geology. Vol. 2, Folds and Faults*. Academic Press, London.

Schmidt, C. J., Genovese, P. W. and Chase, R. B. (1993) Role of basement fabric and cover-rock lithology on the geometry and kinematics of twelve folds in the Rocky Mountain foreland. In *Laramide Basement Deformation in the Rocky Mountain Foreland of the Western United States*, eds C. J. Schmidt, R. B. Chase and E. A. Erslev, Geological Society of America Special Paper **280**, 1–44.

Shaw, E. W. (1963) Canadian Rockies—orientation in time and space. In *Backbone of the Americas*, eds O. E. Childs and B. W. Beebe, pp. 231–242.

Spang, J. H., Evans, J. P. and Berg, R. R. (1985) Balanced cross-sections of small fold-thrust structures. *The Mountain Geologist* **22**, 41–46.

Stewart, K. G. and Alvarez, W. (1991) Mobile-hinge kinking in layered rocks and models. *Journal of Structural Geology* **13**, 243–259.

Stone, D. S. (1984) The Rattlesnake Mountain, Wyoming, debate: a review and critique of models. *The Mountain Geologist* **21**, 37–46.

Stone, D. S. (1986) Seismic profile: South Elk Basin. In *Seismic Expression Structural Styles*, eds A. W. Bally, Vol. 3, pp. 2.20–2.24. American Association of Petroleum Geologists. Studies in Geology 15.

Storti, F. and Salvini, F. (1996) Progressive rollover fault-propagation folding: A possible kinematic mechanism to generate regional scale recumbent folds in shallow foreland belts. *Bulletin of the American Association of Petroleum Geologists* **80**, 174–193.

Suppe, J. (1985) *Principles of Structural Geology*. Prentice Hall, Englewood Cliffs, New Jersey.

Suppe, J. and Medwedeff, D. A. (1984) Fault-propagation folding. *Geological Society of America Abstracts with Programs* **16**, 670.

Suppe, J. and Medwedeff, D. A. (1990) Geometry and kinematics of fault-propagation folding. *Eclogae Geologicae Helvetiae* **83**, 409–454.

Williams, G. and Chapman, T. (1983) Strains developed in the hanging walls of thrusts due to their slip/propagation rate; a dislocation model. *Journal of Structural Geology* **5**, 563–571.

Willis, B. and Willis, R. (1934) *Geological Structures*. McGraw-Hill, New York.